{001}-Textured $Pb(Zr,Ti)O_3$ Thin Films on Stainless Steel by Pulsed Laser Deposition

Juliette Cardoletti,[1, a)] Philipp Komissinskiy,[1] Enrico Bruder,[1] Carl Morandi,[2] and Lambert Alff[1]
[1)]*Institute of Materials Science, Technische Universität Darmstadt, Alarich-Weiss-Straße 2, 64287 Darmstadt, Germany*
[2)]*George W. Woodruff School of Mechanical Engineering, Georgia Institute of Technology, 801 Ferst Drive, Atlanta, GA, 30332, United States*

(Dated: 11 August 2020)

SUPPLEMENTAL INFORMATION

I. SEM CROSS-SECTION

An SEM image of the cross-section of the $PbZr_{0.52}Ti_{0.48}O_3/LaNiO_3/Al_2O_3/Pt/SS304$ heterostructure was performed using a MIRA3-XMH high resolution scanning electron microscope (SEM) by *TESCAN*. The cross-section was accessed by cutting a trench in the sample with a focused ion beam (FIB) after depositing a thick Pt capping layer. The SEM cross-section in Secondary Electron (SE) mode taken with the in-beam detector is presented in Fig. S1.

II. SWITCHING CURRENT VERSUS FIELD HYSTERESIS LOOPS

The switching current versus electric field hysteresis loops at 100 Hz of 200 nm and 400 nm thick PZT layers of $PZT/LNO/Al_2O_3/Pt/SS304$ samples from which the values of the coercive fields E_c were measured are presented in Fig. S2. The datasets used were the same as their respective *P-E* loops plotted in Fig. 5 of the article.

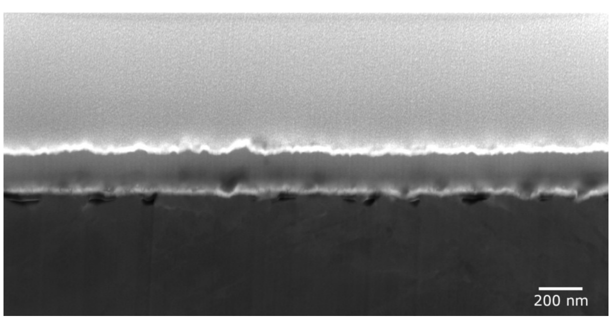

FIG. S1. SEM cross-section of a $PZT/LNO/Al_2O_3/Pt/SS304$ heterostructure, from top to bottom in the SEM image. The image was taken using Secondary Electron (SE) mode with the in-beam detector. The FIB cut creates a "veil" effect on the surface; along with the physical resolution limitations of the SEM, it prevents a clear view of the microstructure. Nevertheless, the image shows porosities at the SS304/Pt interface which is sensitive with the diffusion of Cr from SS304 to Pt leading to the formation of a CrPt phase during the PZT deposition. No porosities can be observed at the other interfaces.

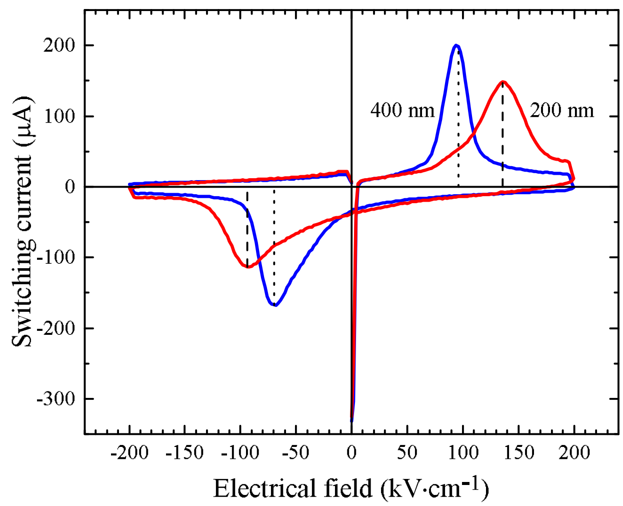

FIG. S2. Switching current versus electric field hysteresis loops at 100 Hz of 200 nm and 400 nm thick PZT layers of $PZT/LNO/Al_2O_3/Pt/SS304$ samples, respectively. The datasets used were the same as their respective *P-E* loops plotted in Fig. 5 of the article. The dashed lines indicates the position of the positive and negative coercive fields of 200 nm and 400 nm thick PZT films, respectively.

III. CONDUCTION MECHANISMS ANALYSIS

The DC leakage current density was fitted according to Schottky emission and to Poole-Frenkel emission, in addition to the space-charge limited current (SCLC) mechanism.

The current density due to Schottky emission can be expressed as[1]:

$$J = A^* T^2 exp\left[\frac{-q(\phi_B - \sqrt{qE/4\pi\varepsilon_r\varepsilon_0})}{kT}\right], \qquad (S1)$$

where J is the current density, A^* is the effective Richardson constant, T is the absolute temperature, q is the electronic charge, $q\phi_B$ is the Schottky barrier height, E is the applied electric field, ε_r is the optical dielectric constant, ε_0 is the permittivity in vacuum, and k is the Boltzmann's constant.

[a)]Electronic mail: juliette.cardoletti@tu-darmstadt.de

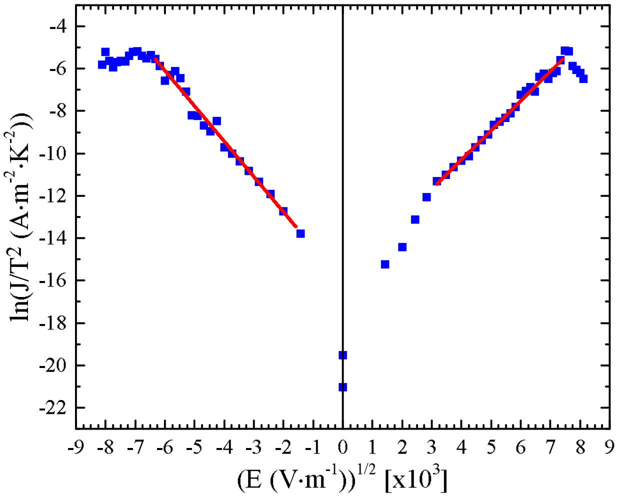

FIG. S3. Leakage current density of the 400 nm thick PZT layer of PZT/LNO/Al_2O_3/Pt/Steel sample (blue squares) plotted for the Schottky emission scenario with a linear fit (red lines) between 100 $\mathrm{kV \cdot cm^{-1}}$ and 550 $\mathrm{kV \cdot cm^{-1}}$ for the positive polarity and between 25 $\mathrm{kV \cdot cm^{-1}}$ and 400 $\mathrm{kV \cdot cm^{-1}}$ for the negative polarity. The absolute values of the slopes of the linear fits are $1.4 \cdot 10^{-3}$ with $R^2 = 0.987$ and $1.7 \cdot 10^{-3}$ with $R^2 = 0.977$ for the positive and negative polarities, respectively.

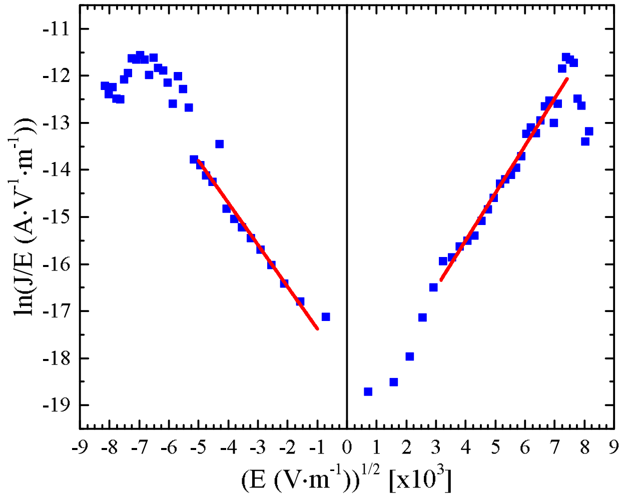

FIG. S4. Leakage current density of the 400 nm thick PZT layer of PZT/LNO/Al_2O_3/Pt/Steel sample (blue squares) plotted for the Poole-Frenkel emission scenario with a linear fit (red lines) between 100 $\mathrm{kV \cdot cm^{-1}}$ and 550 $\mathrm{kV \cdot cm^{-1}}$ for the positive polarity and between 10 $\mathrm{kV \cdot cm^{-1}}$ and 250 $\mathrm{kV \cdot cm^{-1}}$ for the negative polarity. The absolute values of the slopes of the linear fits are $1.0 \cdot 10^{-3}$ with $R^2 = 0.973$ and $8.9 \cdot 10^{-4}$ with $R^2 = 0.945$ for the positive and negative polarities, respectively.

Therefore, when plotting the *I-V* measurements as $ln(J/T^2)$ versus $E^{1/2}$, the slope of the linear region can be used to calculate the optical dielectric constant under the hypothesis of Schottky emission:

$$\varepsilon_r = \frac{q^3}{4\pi\varepsilon_0(slope * kT)^2}. \qquad \text{(S2)}$$

From there, the refractive index, $n = \sqrt{\varepsilon_r}$ can be estimated.

The plot of $ln(J/T^2)$ versus $E^{1/2}$ with a linear fit between 100 $\mathrm{kV \cdot cm^{-1}}$ and 550 $\mathrm{kV \cdot cm^{-1}}$ for the positive polarity and between 25 $\mathrm{kV \cdot cm^{-1}}$ and 400 $\mathrm{kV \cdot cm^{-1}}$ for the negative polarity is presented in Fig. S3. The absolute values of the slopes of the linear fits under the hypothesis of Schottky emission are $1.4 \cdot 10^{-3}$ and $1.7 \cdot 10^{-3}$ for the positive and negative polarities, respectively. It corresponds to $n_S = 1.06$ and $n_S = 0.88$, respectively. According to literature, the refractive index[2] of $PbZr_{0.52}Ti_{0.48}O_3$ is $n_{th.} = 2.2 - 2.7$. The refractive indexes obtained in this work by applying the Schottky emission hypothesis are less than half $n_{th.}$ and, therefore, this hypothesis cannot be validated.

The current density due to Poole-Frenkel emission is expressed by[1]:

$$J = q\mu N_C E exp\left[\frac{-q(\phi_T - \sqrt{qE/\pi\varepsilon_r\varepsilon_0})}{kT}\right], \qquad \text{(S3)}$$

with μ the electronic drift mobility, N_C the density of states in the conduction band, and $q\phi_T$ is the trap energy level.

From this equation, it can be concluded that the slope of the linear region when plotting $ln(J/E)$ versus $E^{1/2}$ can be used to calculate the optical dielectric constant under the hypothesis of Poole-Frenkel emission:

$$\varepsilon_r = \frac{q^3}{\pi\varepsilon_0(slope * kT)^2}. \qquad \text{(S4)}$$

The plot of $ln(J/E)$ versus $E^{1/2}$ with a linear fit between 100 $\mathrm{kV \cdot cm^{-1}}$ and 550 $\mathrm{kV \cdot cm^{-1}}$ for the positive polarity and between 10 $\mathrm{kV \cdot cm^{-1}}$ and 250 $\mathrm{kV \cdot cm^{-1}}$ for the negative polarity is shown in Fig. S4. The absolute values of the slopes of the linear fits under the hypothesis of Poole-Frenkel emission are $1.0 \cdot 10^{-3}$ and $8.9 \cdot 10^{-4}$ for the positive and negative polarities, respectively. It gives refractive indexes for the PZT layer of $n_{PF} = 2.92$ and $n_S = 3.31$, respectively, which are slightly larger than $n_{th.}$ and, therefore, the hypothesis of Poole-Frenkel emission can be neither validated nor dismissed.

While the Schottky emission hypothesis gives a refractive index incoherent with literature values for $PbZr_{0.52}Ti_{0.48}O_3$, the Poole-Frenkel emission hypothesis remains a possibility. Nonetheless, the hypothesis of a SCLC mechanism presented in the article is the most likely of the studied conduction mechanisms.

ACKNOWLEDGMENTS

The authors thank Ulrike Kunz for performing the focused ion beam cut of the sample for the SEM cross-section.

[1] F.-C. Chiu, "A review on conduction mechanisms in dielectric films," Advances in Materials Science and Engineering **2014**, 578168 (2014).

[2]S. Trolier-McKinstry, J. Chen, K. Vedam, and R. E. Newnham, "In Situ Annealing Studies of Sol-Gel Ferroelectric Thin Films by Spectroscopic Ellipsometry," Journal of American Ceramic Society **78**, 1907–1913 (1995).